

Complete DFM Model for High-Performance Computing SoCs with Guard Ring and Dummy Fill Effect

Chun-Chen Liu, Oscar Lau, Jason Y. Du
University of California, Los Angeles yuandu@ucla.edu

Abstract— For nanotechnology, the semiconductor device is scaled down dramatically with additional strain engineering for device enhancement, the overall device characteristic is no longer dominated by the device size but also circuit layout. The higher order layout effects, such as well proximity effect (WPE), oxide spacing effect (OSE) and poly spacing effect (PSE), play an important role for the device performance, it is critical to understand Design for Manufacturability (DFM) impacts with various layout topology toward the overall circuit performance. Currently, the layout effects (WPE, OSE and PSE) are validated through digital standard cell and analog differential pair test structure. However, two analog layout structures: the guard ring and dummy fill impact are not well studied yet, then, this paper describes the current mirror test circuit to examine the guard ring and dummy fills DFM impacts using TSMC 28nm HPM process.

Index Terms — DFM, SoC, WPE, OSE, PSE, high-performance computing, guard ring, dummy fill

I. INTRODUCTION

With advance of nanotechnology, the semiconductor device is scaled down rapidly with additional strain engineering for device enhancement, the overall device characteristic is no longer dominated by the device size but also layout effects (WPE, OSE and PSE) [1]. It is critical to understand Design for Manufacturability (DFM) impacts with various layout topology toward the overall circuit performance. Currently, the digital standard cell and analog differential pair layout test structure are implemented to validate the layout effects. However, two important analog circuit layout topology: guard ring and dummy fill impact are not well studied yet. Therefore, this paper describes a current mirror test circuit to examine the guard ring and dummy fills DFM impacts using TSMC 28nm HPM process.

For analog design, the circuit performance is highly dependent on the device matching, then, the centroid topology is often chosen to minimize the layout environmental variation. The transistors are arranged symmetrically in centroid style where all the devices suffer from the same physical and electrical impacts from all directions. The centroid topology focuses the active devices layout impacts only, the guard ring protection and dummy fill layout structures are not fully taken into consideration yet. At a result, the modified current mirror

configurations are implemented to explore various guard ring and dummy fill DFM impacts.

II. MODIFIED TEST STRUCTURE

In Figure 1, it is shown the conventional current mirror [2] centroid layout topology, the multi-finger devices: MA and MB are placed alternatively and symmetrically, the individual transistor experience same layout impacts, they suffer same physical and electrical impacts from all direction [3]. This layout topology is originally developed to minimize the angular implant doping variation, it is further enforced to reduce layout effects (WPE, OSE and PSE) impacts since 45nm process [4][5]. This paper focuses on the fine centroid layout style rather than the coarse one where a group of transistors are arranged symmetrically to minimize high interconnect RC parasitic impacts.

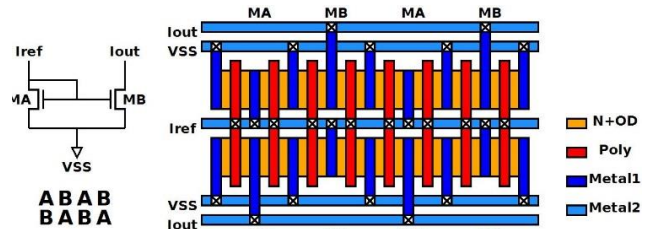


Figure 1. NMOS Current Mirror Fine Centroid Topology

In order to isolate the current mirror from other impacts, the active devices are protected by guard ring and diffusion (OD)/poly (PO) dummy. The guard ring is typically used to protect the active devices from latch-up and noise interference where P+ guard ring with VSS connection protects NMOS active devices, PMOS active devices surrounds with N+ guard ring connected to VDD as shown in Figure 2. There are two kinds of guard ring: single and double guard ring where the single guard ring employs either P+ or N+ guard ring only, the double guard ring mixes with both P+ and N+ guard ring.

Currently, the simulation model only considers the active device layout effect impacts, it ignores the physical and electrical impacts introduced by guard ring. Only diffusion spacing between active devices and guard ring are considered in simulation using OSE model. The guard ring diffusion width and P+/N+ implant type both contribute to the device mobility changes. Therefore, we propose to modify the original OSE

model [6] by introducing effective STI width (STI_{W_{eff}}) parameter. As a first-order model, we set a threshold of OD width of single guard ring (OD_{W_{th}}) when guard ring effect comes into play. The value of OD_{W_{th}} can be found by experiment. If ODW is smaller than OD_{W_{th}}, then the STI_{W_{eff}} is defined as

$$STI_{W_{eff}} = STIW \times \left(1 + K \frac{ODW_{th}}{ODW}\right) \quad (1)$$

where K is curve fitting parameter.

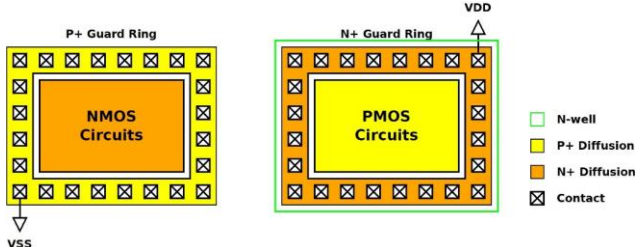


Figure 2. P+/N+ Guard Ring

Dummy fill is typically related with three different type dummy: diffusion, poly and metal. This paper mainly focuses on diffusion (OD) dummy fill because the diffusion uniformity is directly related with Shallow Trench Isolation (STI) and Rapid Temperature Annealing (RTA) process that linked with the transistors formation. The poly (PO) dummy fill is critical for 3D FinFet technology because the height of FinFet is directly dependent on the PO dummy density. Finally, the metal dummy is closely linked to Chemical Mechanical Polishing (CMP) process and directly impacts toward interconnect RC parasitic. For current test chip implementation, it is divided into two level dummy fill. The first level dummy structure is similar to current mirror with same dimension and diffusion type, the second level dummy structure is used to examine different OD fill impacts as shown in Figure 3.

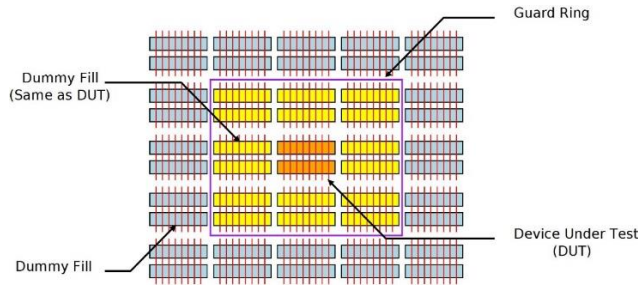


Figure 3. Device under Test (DUT) Structure

Most of OD dummy fill is limited to N+OD dummy fill in order to simplify the chip implementation, it further explores with P+OD and mixed N+OD/P+OD dummy fill impacts toward different current mirror configurations. The conventional fine centroid PMOS/NMOS current mirrors are chosen with N+OD dummy fills as reference circuit for comparison because N+OD dummy fill is commonly offered by foundry. It is easy to implement compared with P+OD and mixed one. For test chip implementation, it focuses on the

different type of diffusion impacts toward current mirror performance. All the poly, diffusion and metal density are same for all test structures, except the type of diffusion. Three type diffusion: N+OD, P+OD are mixed one are implemented. The type of diffusion is highly related with Rapid Temperature Annealing (RTA) process for device threshold voltage and leakage variation [7]. The effect threshold voltage can be expressed as:

$$V_{teff} = V_{tref}(1 + f(D_{NOD}, D_{POD})) \quad (2)$$

where D_{NOD} and D_{POD} are dummy density for N+OD and P+OD within 100 μm x 100 μm window around MOSFETs, respectively, and f(D_{NOD}, D_{POD}) is a look-up table function which is obtained by measurement. Therefore, the test structure is used to study threshold voltage changes with different type of dummy diffusion fills.

III. TEST CHIP RESULTS

In order to validate analog test structure, various current mirrors are implemented using TSMC 28nm HPM process as shown in Figure 4. It includes five PMOS (Table 1) and five NMOS (Table 2) current mirrors. The distance between guard ring and active devices is 1μm. For single guard ring, the OD widths in guard ring are 0.14 μm (1X) and 0.28 μm (2X), respectively. For double guard ring, the OD width is 0.28 μm for both P-type and N-type guard ring. The distance between N-type and P-type guard ring is 0.4 μm. For OD dummy fill, the total OD density is over 50% within 100 μm x 100 μm window. For N+/P+ OD dummy fill, half of OD dummy is P-type and the other half is N-type.

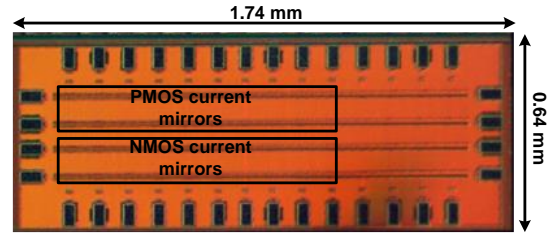


Figure 4. Guard Ring and Dummy Fill Die photo

Type	Guard Ring	Dummy	Simulated Ratio	Measured Ratio
PMOS	Double	P+OD	1.00	1.00
PMOS	Single 1X	P+OD	1.00	1.01
PMOS	Single 2X	P+OD	1.00	1.05
PMOS	Double	N+OD	1.00	0.99
PMOS	Double	N+/P+OD	1.00	0.99

Table 1. PMOS Current Mirror Measurement

From Table 1, the single guard ring has 1%~5% larger current compared with double guard ring because the PMOS guard ring introduces additional tensile stress to enhance mobility, and the tensile stress is further increased with wider guard ring (i.e. 2X). This impact is predicted by proposed modified OSE model. The comparison of simulation with original OSE model, with proposed OSE model and measurement is shown in Fig. 4. For double guard ring, the P+/N+ guard rings offset each other performance enhancement. Regard to different OD fill, the impacts are relatively minor with 1% performance difference. This means

$f(D_NOD, D_POD)$ has small value for PMOS.

Type	Guard Ring	Dummy	Simulated Ratio	Measured Ratio
NMOS	Double	N+OD	1.00	1.00
NMOS	Single 1X	N+OD	1.00	1.01
NMOS	Single 2X	N+OD	1.00	1.05
NMOS	Double	P+OD	1.00	1.09
NMOS	Double	N+/P+OD	1.00	1.10

Table 2. NMOS Current Mirror Measurement

From Table 2, NMOS current mirror performance is different from PMOS one due to compressive stress that degrades the device driving capability. The single guard ring shows the performance enhancement similar to PMOS one. P+OD and mixed OD dummy fills increase the current by about 10%.

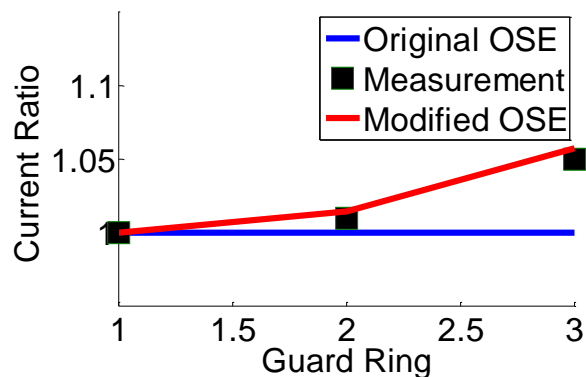


Figure 5. Comparison of original OSE model, measurement and modified OSE model

IV. CONCLUSION

The guard ring and OD dummy fill effect on performance of MOSFET is studied in this paper. The silicon measurement and simulation result difference is as high as 10% with guard ring and dummy fill, compared the original model with the modified model. The preliminary guard ring and OD dummy fill models are proposed to improve the simulation accuracy. For future development, more test keys are requirement to estimate the OD density gradient impacts and how to apply guard ring to protect the active circuit from the neighbor passive resistor and capacitor.

REFERENCES

- [1] A. Woo, H. Eberhart, Y. Li, and A. Ito, Mismatch in High-K Metal Gate Process Analog Design, IEEE International Electron Devices Meeting, 18.2.1-8.2.4, 2015
- [2] B. Razavi, Design of Analog CMOS Integrated Circuits, McGraw-Hill, 2001.
- [3] A. Hastings, The Arts of Analog Layout, 2nd Edition, Prentice Hall, 2006.
- [4] K. Kuhn, C. Kenyon, A. Kornfeld, M. Liu, A. Maheshwari, W.K. Shih, S. Sivakumar, G. Taylor, P. VanDerVoorn and K. Zawadzki, Managing Process Variation in Intel's 45nm CMOS Technology, Intel Technology Journal, Volume 12, Issue 2008, p.93-109.
- [5] Clair Webb, 45nm Design for Manufacturing, Intel Technology Journal, Volume 12, Issue 2008, p.121-130.
- [6] J. Xue, Z. Ye, Y. Deng, H. Wang and Z. Yu, Layout-Dependent STI Stress Analysis and Stress-Aware RF/Analog Circuit Design Optimization, ICCAD 2009, p.521-p.528
- [7] Y. Wei, J. Hu, Frank Liu and S.S. Sapatnekar, Physical Design Techniques for Optimizing RTA-induced Variations, ISPD 2010, 9A

- [8] J. Jaussi et al., "26.2 A 205mW 32Gb/s 3-Tap FFE/6-tap DFE bidirectional serial link in 22nm CMOS," 2014 IEEE International Solid-State Circuits Conference Digest of Technical Papers (ISSCC), San Francisco, CA, 2014, pp. 440-441.
- [9] B. Hu et al., "A Capacitor-DAC-Based Technique For Pre-Emphasis-Enabled Multi-Level Transmitters," in IEEE Transactions on Circuits and Systems II: Express Briefs, vol. PP, no.99, pp.1-1
- [10] Y. Du et al., "A 16Gb/s 14.7mW tri-band cognitive serial link transmitter with forwarded clock to enable PAM-16 / 256-QAM and channel response detection in 28 nm CMOS," 2016 IEEE Symposium on VLSI Circuits (VLSI-Circuits), Honolulu, HI, 2016, pp. 1-2.
- [11] Y. Du et al., "A 16-Gb/s 14.7-mW Tri-Band Cognitive Serial Link Transmitter With Forwarded Clock to Enable PAM-16/256-QAM and Channel Response Detection," in IEEE Journal of Solid-State Circuits, vol. PP, no.99, pp.1-12
- [12] Du, Yuan. (2016). Cognitive Serial Interface with Multi-Band Signaling and Channel Learning Mechanism. UCLA: Electrical Engineering 0303. Retrieved from: <http://escholarship.org/uc/item/8vs373c5>
- [13] W. H. Cho et al., "A 5.4-mW 4-Gb/s 5-band QPSK transceiver for frequency-division multiplexing memory interface," 2015 IEEE Custom Integrated Circuits Conference (CICC), San Jose, CA, 2015, pp. 1-4.
- [14] Y. Li et al., "Carrier synchronisation for multiband RF interconnect (MRFI) to facilitate chip-to-chip wireline communication," in Electronics Letters, vol. 52, no. 7, pp. 535-537, 2016.
- [15] W. H. Cho et al., "A 38mW 40Gb/s 4-lane tri-band PAM-4 / 16-QAM transceiver in 28nm CMOS for high-speed Memory interface," 2016 IEEE International Solid-State Circuits Conference (ISSCC), San Francisco, CA, 2016, pp. 184-185.
- [16] H. Wu et al., "A Current-Mode mm-Wave direct-conversion receiver with 7.5GHz Bandwidth, 3.8dB minimum noise-figure and +1dBm P1dB, out linearity for high data rate communications," 2013 IEEE Radio Frequency Integrated Circuits Symposium (RFIC), Seattle, WA, 2013, pp. 89-92.
- [17] Z. Z. Chen et al., "A wide-band 65nm CMOS 28-34 GHz synthesizer module enabling low power heterodyne spectrometers for planetary exploration," 2015 IEEE MTT-S International Microwave Symposium, Phoenix, AZ, 2015, pp. 1-3.
- [18] H. Wu, N. Y. Wang, Y. Du and M. C. F. Chang, "A Blocker-Tolerant Current Mode 60-GHz Receiver With 7.5-GHz Bandwidth and 3.8-dB Minimum NF in 65-nm CMOS," in IEEE Transactions on Microwave Theory and Techniques, vol. 63, no. 3, pp. 1053-1062, March 2015.
- [19] Y. Li et al., "A multi-band low-noise transmitter with digital carrier leakage suppression and linearity enhancement," in IEEE Transactions on Circuits and Systems I: Regular Papers, vol. 60, no. 5, pp. 1209-1219, May 2013.
- [20] Lv Jingjing Du Li, "Vehicular Collision Avoiding System Based on Two Ultrasonic Receivers," Value Engineering, vol. 22, 2010.
- [21] L. Du et al., "A 2.3 mW 11 cm Range Bootstrapped and Correlated Double Sampling 3D Touch Sensing Circuit for Mobile Devices," in IEEE Transactions on Circuits and Systems II: Express Briefs, 2017.
- [22] L. Du et al., "A 2.3mW 11cm-range bootstrapped and correlated-double-sampling (BCDS) 3D touch sensor for mobile devices," 2015 IEEE International Solid-State Circuits Conference - (ISSCC) Digest of Technical Papers, San Francisco, CA, 2015
- [23] L. Du et al., "Invited--Airtouch: A novel single layer 3D touch sensing system for human/mobile devices interactions," 2016 53rd ACM/EDAC/IEEE Design Automation Conference (DAC), Austin, TX, 2016, pp. 1-6.
- [24] A. Tang et al., "A 95 GHz centimeter scale precision confined pathway system-on-chip navigation processor for autonomous vehicles in 65nm CMOS," 2015 IEEE MTT-S International Microwave Symposium, Phoenix, AZ, 2015, pp. 1-3.
- [25] A. Tang et al., "CMOS (Sub)-mm-Wave System-on-Chip for exploration of deep space and outer planetary systems," Proceedings of the IEEE 2014 Custom Integrated Circuits Conference, San Jose, CA, 2014, pp. 1-4.
- [26] A. Tang et al., "A 65nm CMOS 140 GHz 27.3 dBm EIRP transmit array with membrane antenna for highly scalable multi-chip phase arrays," 2014 IEEE MTT-S International Microwave Symposium (IMS2014), Tampa, FL, 2014, pp. 1-3.
- [27] A. Tang et al., "A 200 GHz 16-pixel focal plane array imager using CMOS super regenerative receivers with quench synchronization," 2012 IEEE/MTT-S International Microwave Symposium Digest, Montreal, QC, Canada, 2012, pp. 1-3.

- [28] Y. Zhao et al., "A 0.56 THz Phase-Locked Frequency Synthesizer in 65 nm CMOS Technology," in *IEEE Journal of Solid-State Circuits*, vol. 51, no. 12, pp. 3005-3019, Dec. 2016.
- [29] R. Al Hadi, Y. Zhao, Y. Li, Y. Du, and M.-F. Chang, "Retroactive Terahertz Displacement Sensor in a standard 65nm CMOS Technology," in *Conference on Lasers and Electro-Optics, OSA Technical Digest (2016)* (Optical Society of America, 2016), paper STh3I.3.
- [30] R. A. Hadi et al., "A spectral profiling method of mm-wave and terahertz radiation sources," 2016 IEEE MTT-S International Microwave Symposium (IMS), San Francisco, CA, 2016, pp. 1-3.
- [31] <http://www.itrs2.net/itrs-reports.html>
- [32] Jason Cong, Mohammad Ali Ghodrati, Michael Gill, Beayna Grigorian, Karthik Gururaj, and Glenn Reinman. 2014. Accelerator-Rich Architectures: Opportunities and Progresses. In *Proceedings of the 51st Annual Design Automation Conference (DAC '14)*. ACM, New York, NY, USA, Article 180, 6 pages
- [33] Voutilainen, M., Rouvala, M., Kotiranta, P., & von Rauner, T. (2009). Multi-gigabit serial link emissions and mobile terminal antenna interference. *IEEE Workshop on Signal Propagation on Interconnects (SPI)* (pp. 1-4).
- [34] B. Mutnury, F. Paglia, J. Mobley, G. K. Singh and R. Bellomio, "QuickPath Interconnect (QPI) design and analysis in high speed servers," 19th Topical Meeting on Electrical Performance of Electronic Packaging and Systems, Austin, TX, 2010, pp. 265-268.
- [35] <https://www.rogerscorp.com/>